

# An Autoadaptive Edge-Detection Algorithm for Flame and Fire Image Processing

Tian Qiu, Yong Yan, *Fellow, IEEE*, and Gang Lu, *Senior Member, IEEE*

**Abstract**—The determination of flame or fire edges is the process of identifying a boundary between the area where there is thermochemical reaction and those without. It is a precursor to image-based flame monitoring, early fire detection, fire evaluation, and the determination of flame and fire parameters. Several traditional edge-detection methods have been tested to identify flame edges, but the results achieved have been disappointing. Some research works related to flame and fire edge detection were reported for different applications; however, the methods do not emphasize the continuity and clarity of the flame and fire edges. A computing algorithm is thus proposed to define flame and fire edges clearly and continuously. The algorithm detects the coarse and superfluous edges in a flame/fire image first and then identifies the edges of the flame/fire and removes the irrelevant artifacts. The autoadaptive feature of the algorithm ensures that the primary symbolic flame/fire edges are identified for different scenarios. Experimental results for different flame images and video frames proved the effectiveness and robustness of the algorithm.

**Index Terms**—Edge detection, feature extraction, fire, flame, image edge analysis, image processing, monitoring, shape measurement.

## I. INTRODUCTION

TO MEET the stringent standards on combustion efficiency and pollutant emissions, quantitative flame monitoring is becoming increasingly important in fossil-fuel-fired combustion systems, particularly in power generation plants [1]. This has led to a wave of research on advanced flame imaging technologies [2], [3] both in the power generation industry and in laboratory research. In fire safety engineering, flame image processing is also emphasized as image-based flame detectors are increasingly applied in fire detection systems [4]–[9]. Compared to conventional flame detectors such as those based on optical sensing, ionization current detection, and thermocouple, image-based flame detectors are deemed more appropriate in fire detection because of their capability for remote detection of a small-sized fire, as well as having other advantages [10].

As one of the important steps in flame and fire image processing, edge detection is often the precursor and lays a foundation for other processing. There are several reasons why

it is necessary to identify flame edges. First, the flame edges form a basis for the quantitative determination of a range of flame characteristic parameters such as shape, size, location, and stability. Second, the definition of flame edges can reduce the amount of data processing and filter out unwanted information such as background noise within the image. In other words, edge detection can preserve the important structural properties of the flame and meanwhile shorten the processing time. Third, edge detection can be used to segment a group of flames. This is helpful for multiple flame monitoring in some industrial furnaces where a multiburner system is used. Furthermore, timely determination of flame edges can trigger a fire alarm and provide the fire fighters with information on fire type, combustible substances, exterior of the flame, etc. For instance, the movement of a detected flame edge can be used to distinguish real and false fire alarms [11].

A number of methods have been reported for identifying flame edges for the geometric characterization of a flame [12], [13] or fire [14], [15]. Adkins [16] developed a software tool to analyze fire images, with which one can use a mouse to trace the flame edge. It is a manual edge-detection method, but it does show the importance and usefulness of the flame/fire edge detection. Bheemul *et al.* [13] introduced an effective method to extract flame contours by detecting the changes of the brightness in the horizontal direction line by line over a flame image, but the method is only suitable for simple and steady flames. Zhang *et al.* [5] presented a new method using FFT and wavelet transform for the contour analysis of forest fire images on a video. Lu *et al.* [6] proposed an algorithm for early fire detection and tested it on video clips. Toreyin *et al.* [7], [8], [11] succeeded in detecting the fire in a real-time video using different methods such as hidden Markov models and wavelet transform. Chacon-Murguia and Perez-Vargas [9] managed to detect and analyze fire information on a video through the analysis of shape regularity and intensity saturation feature. Razmi *et al.* [10] used a background subtraction and Prewitt edge-detection approach to detecting flames for fire protection systems. She and Huang [17] proposed a Chan–Vese active contour model for the edge detection of flames in a power plant. Jiang and Wang [15] also demonstrated an improved Canny edge detector which was used to detect moving fire regions in large space fire images. Although each of these methods has its own advantages for the given tasks, such as fire detection or shape reconstruction in a complex background, or helping to detect an early fire and trigger a fire alarm, they have some limitations. For instance, some flame edges detected are unclear, discontinuous, or do not well match the actual flame shape. For the purpose of detecting the flame’s size and shape and, consequently, the

Manuscript received June 20, 2011; revised September 9, 2011; accepted October 11, 2011. Date of publication December 30, 2011; date of current version April 6, 2012. This work was supported by the Research Councils U.K.’s Energy Program under Grants EP/G062153/1 and EP/G063214/1. The Associate Editor coordinating the review process for this paper was Dr. Zheng Liu.

The authors are with the Instrumentation, Control and Embedded Systems Research Group, School of Engineering and Digital Arts, University of Kent, CT2 7NT, Canterbury, Kent, U.K. (e-mail: t.qiu@kent.ac.uk; y.yan@kent.ac.uk; g.lu@kent.ac.uk).

Color versions of one or more of the figures in this paper are available online at <http://ieeexplore.ieee.org>.

Digital Object Identifier 10.1109/TIM.2011.2175833

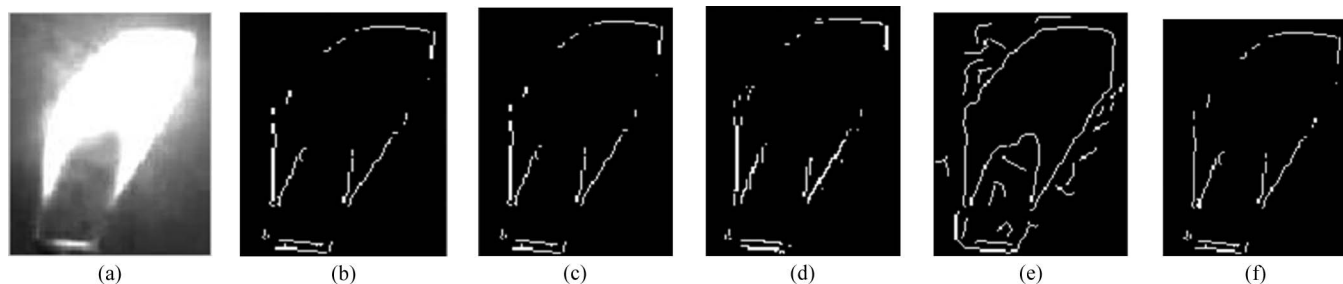


Fig. 1. Representative results using the common edge-detection methods and Laplacian method. (a) Original image. (b) Sobel method. (c) Prewitt method. (d) Roberts method. (e) Canny method. (f) Laplacian method.

geometric characteristics, it is necessary to attain the clear, continuous and, where possible, closed edge of the flame.

In this paper, several conventional edge-detection methods have been examined to assess their effectiveness in flame edge identification. Despite the delicate adjustment of many parameters in the use of these methods, the results were still unsatisfactory. Edges extracted from nontrivial images are often hampered by fragmentation, meaning that the edge curves are not connected, edge segments are melted, or false edges that do not correspond to significant phenomena in the image are shown. It is therefore desirable to develop a dedicated edge-detection method for flame and fire image processing. Accordingly, a new computing algorithm is proposed in this paper to process a combustion image and to identify flame/fire edges.

Section I of this paper is a background introduction and a brief literature review of flame edge-detection methods. Section II discusses related edge-detection methods and their application to flame images. Section III proposes a new methodology of detecting edges of flame images with a detailed description of each step. Section IV presents experimental results and gives some examples of how to use the detected edges for characterizing flames. Concluding remarks and a scope for further research are given in Section V. The basic methodology that is applied to develop the algorithms, together with preliminary results, was reported at the 2011 IEEE International Instrumentation and Measurement Technology Conference [25]. This paper presents a detailed description of the methodology that has been developed along with the improvement of the algorithm, more experimental results, and detailed discussions.

## II. CONVENTIONAL METHODS OF EDGE DETECTION AND THEIR APPLICATIONS TO FLAME IMAGES

A typical edge in an image might, for instance, be the border between blocks of different colors or different gray levels. Mathematically, the edges are represented by first- and second-order derivatives. The first-order derivative (i.e., gradient) of a 2-D function  $f(x, y)$  is defined as vector [18]

$$\nabla f = \begin{bmatrix} G_x \\ G_y \end{bmatrix} = \begin{bmatrix} \frac{\partial y}{\partial x} \\ \frac{\partial y}{\partial x} \end{bmatrix} \quad (1)$$

where  $G_x$  and  $G_y$  are the gradients in the  $x$  and  $y$  coordinates, respectively. The magnitude of the vector is given by

$$mag(\nabla f) = \sqrt{G_x^2 + G_y^2} = \sqrt{\left(\frac{\partial y}{\partial x}\right)^2 + \left(\frac{\partial y}{\partial x}\right)^2}. \quad (2)$$

The angle  $\alpha$  at which the maximum rate of change occurs is

$$\alpha(x, y) = \tan^{-1} \left( \frac{G_y}{G_x} \right). \quad (3)$$

Generally, the variance of the gray level is calculated with one of these edge-detection operators or kernel operators. The slopes in the  $x$ - and  $y$ -directions are combined to give the total value of the edge strength. The edge-detection operator is then calculated by forming a matrix centered on a pixel chosen as the center of the matrix area. If the value of this matrix area is above a given threshold, then the middle pixel is classified as an edge [18].

The edge-detection methods that have been published may be grouped into two categories according to the computation of image gradients, i.e., the first-order or second-order derivatives. In the first category, edges are detected through computing a measure of edge strength with a first-order derivative expression. Examples of gradient-based edge-detection operators include Roberts, Prewitt, and Sobel operators [23]. The Canny edge-detection algorithm [20], an improved method using the Sobel operator, is known to be a powerful edge-detection method. In the second category, edges are detected by searching a second-order derivative expression over the image, usually the zero crossings of the Laplacian or a nonlinear differential expression.

In the present research, these common edge-detection methods have been applied with appropriate parameters to process typical flame images. Despite many parameters being finely and appropriately adjusted in the use of these methods, flame edges could not be clearly identified. Fig. 1(a)–(f) shows examples of results obtained by the conventional edge-detection methods along with the original image. The expected flame edge should be one and only one clear, continuous, and uninterrupted edge. However, as the results have shown, the edges identified using these methods are often disconnected and fragmented [Fig. 1(b)–(f)]; some of the methods can only identify a part of the flame edge [Fig. 1(b)–(d)] or wrongly identify small edges that are obviously not the edges of the main flame [Fig. 1(e)]. The results have therefore suggested that it is not always possible to obtain ideal edges from real-life images of moderate complexity, thus complicating the subsequent task of interpreting the image data.

There are some other algorithms proposed for the flame/fire edge detection for various applications [10]–[17]. Although we are unable to test all these methods, the published results have shown that these methods are not suitable for our purpose.

It is therefore desirable to develop a dedicated edge-detection method for flame/fire image processing.

### III. NEW EDGE-DETECTION ALGORITHM FOR FLAME IMAGE PROCESSING

In general, a flame region has a stronger luminance in comparison to its ambient background, and the boundary between the flame region and its background is mostly continuous. Furthermore, in most cases, there is only a main flame in the image; otherwise, the image can be segmented so that each segmented area contains only one main flame. Accordingly, a computing algorithm is proposed where these features are used to identify flame edges. The basic strategy is to detect the coarse and superfluous edges in a flame image then identify the flame's principal edges and remove irrelevant ones. The algorithm can be divided into the following logical steps.

Step 1) *Adjusting the gray level of a flame image.* The first step is to adjust the gray level of a flame image according to its statistical distribution. Considering a discrete grayscale image  $x$  and letting  $n_i$  be the number of occurrences of gray level of  $i$ , the probability of the occurrence of a pixel of gray level  $i$  in the image is [21]

$$P_x(i) = p(x = i) = \frac{n_i}{n}, \quad 0 < i < L \quad (4)$$

where  $L$  is the total number of gray levels in the image,  $n$  the total number of pixels in the image, and  $p_x(i)$  the histogram for pixels with  $i$ , normalized to  $[0,1]$ . Also, the cumulative distribution function (CDF) corresponding to  $p_x$  can be defined as

$$\text{CDF}_x(i) = \sum_{j=0}^i p_x(j) \quad (5)$$

which is also the accumulated normalized histogram of the image.

Next, create a transformation of form  $y = T(x)$  to produce a new image  $\{y\}$ , such that its CDF will be linearized across the value range with a constant number  $K$ , i.e.

$$\text{CDF}_y(i) = iK. \quad (6)$$

To map the values back to their original range, the following transformation is applied to the result

$$y' = y \times (\max\{x\} - \min\{x\}) + \min\{x\}. \quad (7)$$

Step 2) *Smoothing the image to eliminate noise.* The second step is to filter out any noise in the image before locating and detecting any edges. A Gaussian filter can be achieved using a simple mask. Gaussian smoothing [26] is performed using standard convolution methods after a suitable mask is selected. The larger the width of the Gaussian mask, the lower the detector's sensitivity to the background noise in the flame/fire image, but a large mask may also make the detected flame/fire edge so precise that the localization error in the detected flame/fire edges also

|   |    |    |    |   |
|---|----|----|----|---|
| 2 | 4  | 5  | 4  | 2 |
| 4 | 9  | 12 | 9  | 4 |
| 5 | 12 | 15 | 12 | 5 |
| 4 | 9  | 12 | 9  | 4 |
| 2 | 4  | 5  | 4  | 2 |

Fig. 2. Discrete approximation to Gaussian function.

increases slightly with the Gaussian width. After certain tests and comparison, the Gaussian mask, as shown in Fig. 2, is used in the implementation.

Step 3) *Using the Sobel operator for finding basic edges.* Finding basic edges is achieved by finding the gradients of all the pixels in the image so as to highlight the regions with high gray level contrast at their edges. The algorithm then tracks the edge along these regions and suppresses any pixels that are not at the peaks of the gradients. If the magnitude of the gradient is above high threshold  $T_H$ , it is deemed an edge. Moreover, if the magnitude is between the two thresholds, i.e., the  $T_H$  and  $T_L$  (low threshold), it is set to zero unless there is a path from this pixel to a pixel with a gradient above the  $T_L$ .

The Sobel operator performs a 2-D spatial gradient measurement over the image. Then, the approximate absolute gradient magnitude (edge strength) at each point can be found. It uses a pair of  $3 \times 3$  convolution masks, one estimating the gradient in the  $x$ -direction (columns) and another estimating the gradient in the  $y$ -direction (rows). The Sobel operator is expressed as follows [18]:

$$M_x = \begin{bmatrix} -1 & 0 & 1 \\ -2 & 0 & 2 \\ -1 & 0 & 1 \end{bmatrix} \quad (8)$$

$$M_y = \begin{bmatrix} -1 & -2 & -1 \\ 0 & 0 & 0 \\ 1 & 2 & 1 \end{bmatrix}. \quad (9)$$

Step 4) *Adjusting  $T_H$  and  $T_L$  for better results.* Better results are achieved by giving the first pair of  $T_H$  and  $T_L$  initial values according to the *a priori* results of similar flame images and then adjusting the values for a better result. The "better" result is assessed by how many edges there are: The more edge pixels detected in the edge image, the better the parameters are. Another threshold  $T_E$  is also set to restrict the total number of edges, i.e., if the number of edge pixels exceeds the  $T_E$ , the automatic adjustment will be terminated. At this point, a preliminary image with edges identified is obtained from the original flame image. It is designated as a preliminary edge image (PEI).

Step 5) Removing unrelated edges in the PEI.

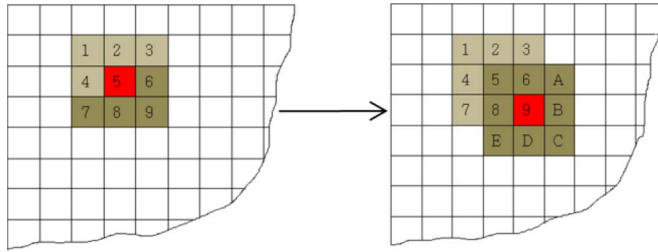


Fig. 3. Illustration of movement of the edge search.

- a) Select any edge point in the PEI, remove that point from the PEI, allocate a new temporary edge image, and plot the point onto the temporary edge image.
- b) Use the selected point as the center, and search in a  $3 \times 3$  area. Store the location of all the neighboring pixels if they are edge pixels. In eight neighboring pixels, operations are taken for the following three different cases.
  - i) If there is no neighboring pixel, the selected point is an isolated point and should be removed from the PEI. Terminate the search, and go to Step 5d).
  - ii) If there is one neighboring pixel, the selected point is an endpoint. It should then be removed from the PEI, plotted onto the temporary edge image, and added into the endpoint list. Start the new search from the found neighbor, and go to Step 5c).
  - iii) If there are two or more than two neighboring pixels, the selected point is a normal transition point in an edge line or an intersection with more than three bifurcations. Set one of the neighboring points as the new search center, and start a new search. Store the other positions as unchecked conjunction points, and then, go back to Step 5b).
- c) Check the conjunction points. If all the conjunction points have been searched as a center, one temporary edge image is then completed. Compute the lengths of any two endpoints in the temporary edge image, and pick out the longest one. Then, go to Step 5d).
- d) If all the pixels in the PEI are moved to the temporary edge image, then go to Step 6).

Fig. 3 shows how the tracing step moves forward if the old search center is replaced by a new search center. For instance, in the left image of the figure, pixel “5” is the center selected. Suppose that an edge point at pixel “9” is found, then remove pixel “5” from the PEI to the temporary edge image, and pixel “9” will be the new search center. In this way, the search moves forward pixel by pixel.

- c) Check the conjunction points. If all the conjunction points have been searched as a center, one temporary edge image is then completed. Compute the lengths of any two endpoints in the temporary edge image, and pick out the longest one. Then, go to Step 5d).
- d) If all the pixels in the PEI are moved to the temporary edge image, then go to Step 6).

Step 6) *Achieving a clearly defined edge.* Select the pixels of the longest edge in the final edge image which should have the same size as the original image. The flowchart of the whole process is shown in Fig. 4.

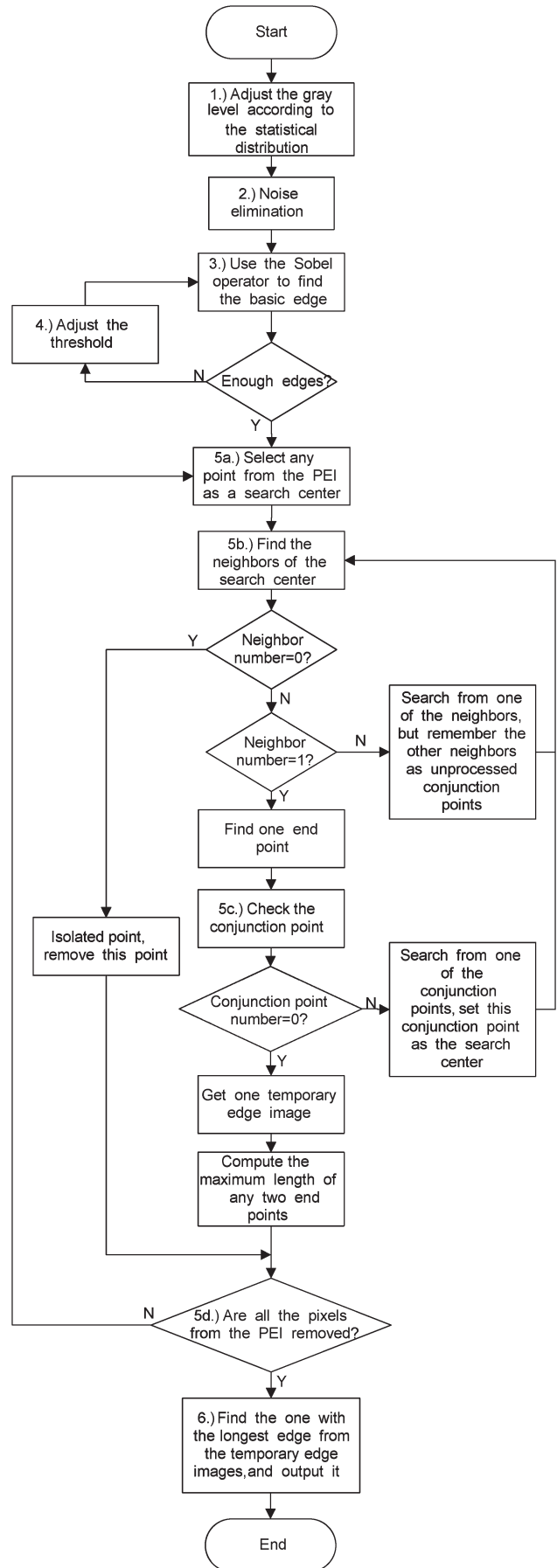


Fig. 4. Flowchart of the flame edge-detection algorithm.

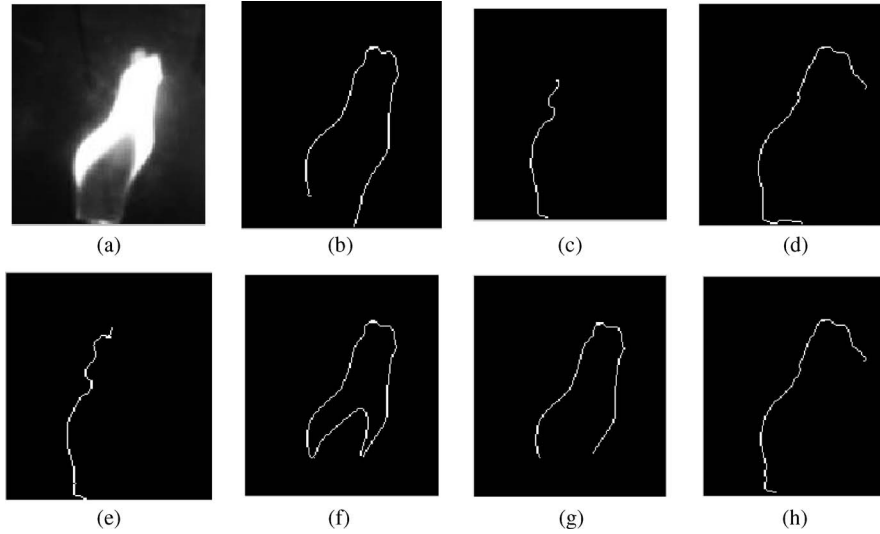


Fig. 5. Illustration of longest curve in a flame image with minimum  $D$ . (a) Original image. (b)  $T_L = 0.098, T_H = 0.98$ . (c)  $T_L = 0.098, T_H = 0.29$ . (d)  $T_L = 0.098, T_H = 0.49$ . (e)  $T_L = 0.2, T_H = 0.29$ . (f)  $T_L = 0.39, T_H = 0.98$ . (g)  $T_L = 0.49, T_H = 0.98$ . (h)  $T_L = 0.2, T_H = 0.49$ .

In order to speed up the process of finding proper  $T_H$  and  $T_L$ , a least mean square (LMS) algorithm is used, which is a class of adaptive filters by finding the filter coefficients that relate to producing the LMS of the error signal between the desired result and the actual result. The idea is to use steepest descent to find filter weights which minimize a cost function. From the method of the steepest descent, the weight vector equation is given by [24]

$$w(n + 1) = w(n) + \frac{1}{2}\mu [-\nabla (E \{e^2(n)\})] \quad (10)$$

where  $\mu$  is the step-size parameter which controls the convergence characteristics of the LMS algorithm and  $e^2(n)$  is the mean square error between the former output  $y(n)$  and the reference signal which is given by

$$e^2(n) = [d^*(n) - w^h x(n)]^2. \quad (11)$$

The gradient vector in the aforementioned weight update equation can be computed as

$$\nabla_w (E \{e^2(n)\}) = -2r(n) + 2R(n) \quad (12)$$

where  $r(n)$  and  $R(n)$  are covariance matrices which are defined as follows:

$$r(n) = x(n)d^*(n) \quad (13)$$

$$R(n) = x(n)x^h(n). \quad (14)$$

Moreover, the weight update can be given by

$$w(n + 1) = w(n) + \mu x(n) [d^*(n) - x^h(n)w(n)] \quad (15)$$

so

$$w(n + 1) = w(n) + \mu x(n)e^*(n). \quad (16)$$

In this application, the two parameters  $T_H$  and  $T_L$  need to be autoadjusted. Give initial  $T_H$  and  $T_L$  according to the *a priori* results, and set one of the parameters as fixed in order to adjust the other one. For example, suppose that  $T_H$  is fixed, then  $T_L$  is adjusted in every step. The Euclidean distance of a curve's start point  $C_s$  and endpoint  $C_e$ , noted as  $D$ , is used as the

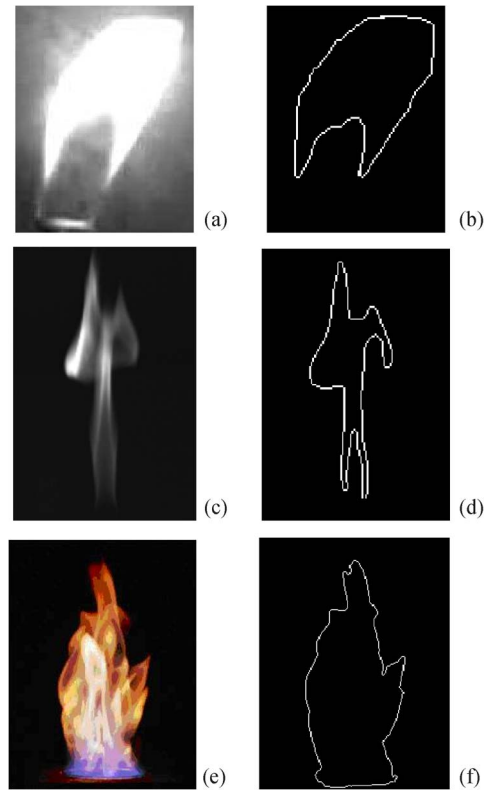


Fig. 6. Some of the flame edge-detection results. (Left column) Original images. (Right column) Images with identified edges. (a) Diffusion propane flame. (c) Partially premixed propane flame. (e) Small-scale pool fire [17]. Note that the image in (a) is reproduced from Fig. 1.

output to judge the effectiveness of the new  $T_L$ . The coordinates of  $C_s(S_x, S_y)$  and endpoint  $(E_x, E_y)$  should be stored in the memory in the tracing process. Thus,  $D$  can be computed as

$$D = \sqrt{(E_x - S_x)^2 + (E_y - S_y)^2}. \quad (17)$$

After the LMS computation process, a suitable  $T_L$  is chosen. If  $D$  is small enough, the computation process terminates; if  $D$  is still greater than the desired value, a further LMS computation process is applied to  $T_H$ .

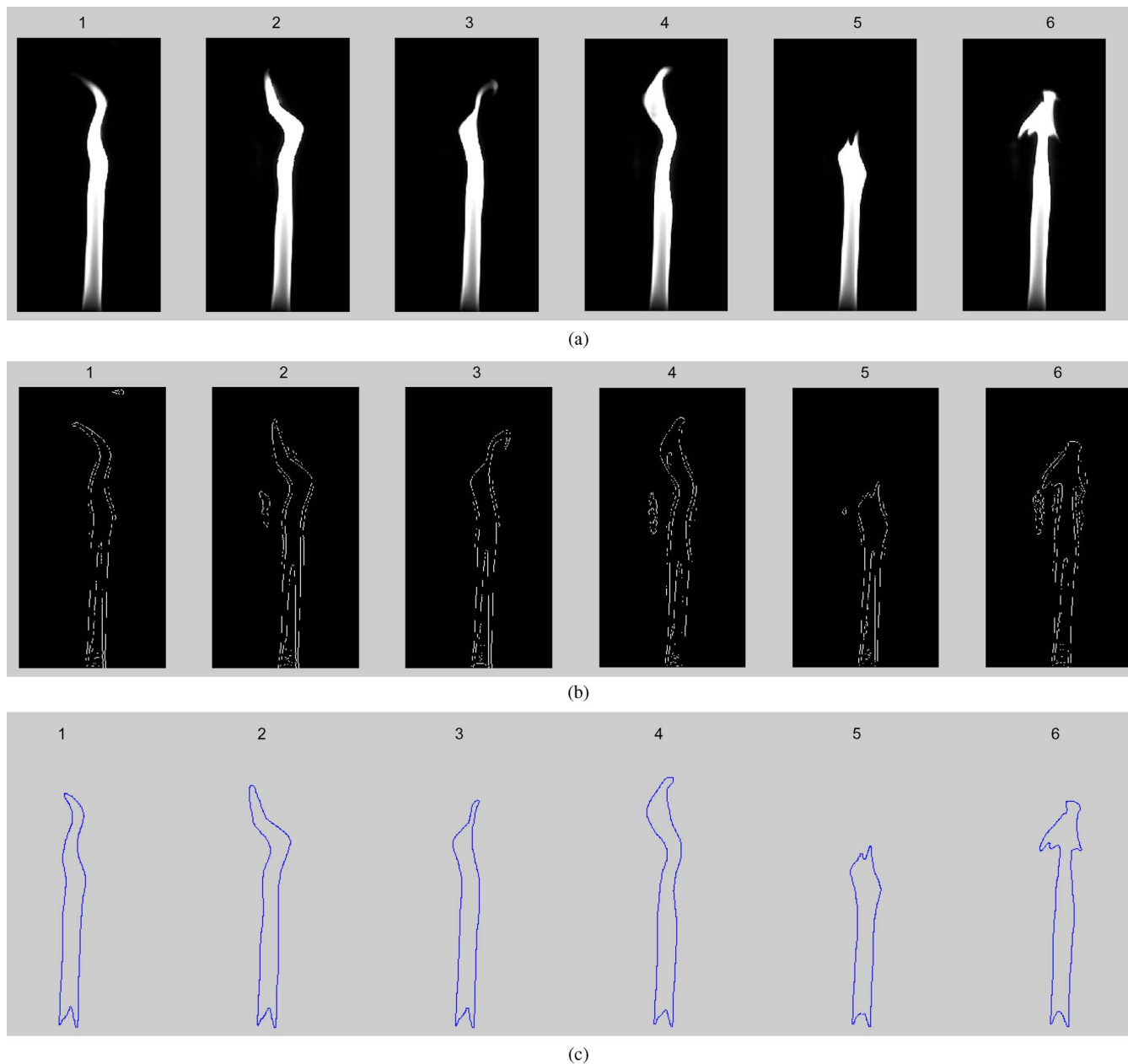


Fig. 7. Edge-detection result for a flame video. (a) Frames in a flame video. (b) Detected flame edge from the video sequence using the Canny edge-detection method. (c) Detected flame edge from the video sequence using the proposed method.

Fig. 5 shows some of the results with the proposed method given the fixed  $T_H$  and  $T_L$ . It can be seen that a pair of proper thresholds is necessary for the integrated flame edge. As explained in Step 4), the first pair of  $T_H$  and  $T_L$  values is selected according to the *a priori* results of similar flame images. The *a priori*  $T_H$  and  $T_L$  will work in most situations, but there are exceptions as the scenario may change and the flame may change enough to make the previous threshold invalid. Fig. 5(f) shows a closed curve, and the Euclidean distance between the start point and the endpoint is zero, which is regarded as the best result in the checked  $T_H$  and  $T_L$  region. Obviously, if  $D = 0$ , no other adjustment of  $T_H$  and  $T_L$  is necessary; thus, the autoadaptive process is over. If  $D$  is still big enough, as that in the situation of Fig. 5(c) and (e), a further adjustment has to be executed. The  $T_H$  and  $T_L$  should be adjusted in a greater

scale. When  $D$  becomes very small, for example, less than 20 pixels, the  $T_H$  and  $T_L$  should be adjusted through finer steps.

#### IV. RESULTS AND DISCUSSIONS

After implementing the algorithm as described in Section III, thousands of flame images were processed using the algorithm so as to evaluate its effectiveness. Most of the flame images were taken for propane Bunsen flames burning in open air. Some of the images were attained from the Internet with courtesy of permission of use. The desktop computer used has a 2.66-GHz Intel Quad CPU and can detect the edges of about 120 flame images of  $141 \times 161$  pixels in 1 min. Fig. 6 shows typical processed flame images with edges identified. In comparison with the test results shown in Fig. 1, it can be clearly

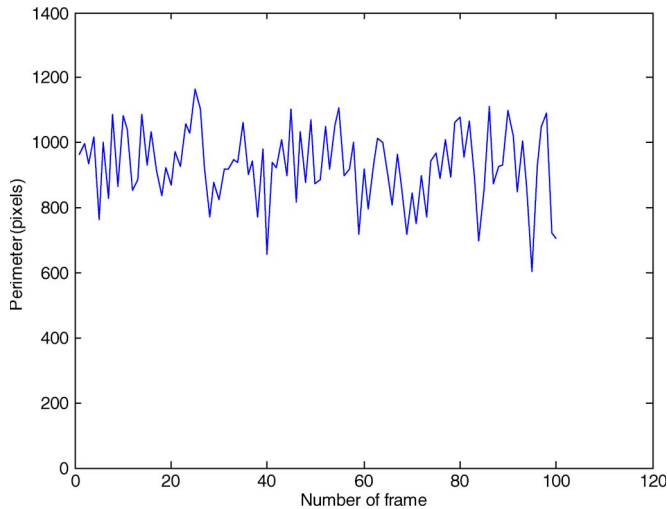


Fig. 8. Uninterrupted computing of the flame perimeters from a flame video.

observed that the developed algorithm can successfully detect clear edges of the flame and disregard unrelated artifacts, which common edge-detection methods cannot achieve. The proposed method makes it much easier to distinguish the flame region from the background. The algorithm can also be used to extract the edges of more complex flames such as turbulent diffusion flames or flames of pool fires [14]. The clearly defined flame edges will form a basis for subsequent processing of the flame images, for example, flame size computation, flame background removal, and determination of other flame parameters [3].

Many flame videos are also tested for continuous edge detection so as to evaluate the robustness of the system. Fig. 7(a) shows a series of frames acquired from a flame video. Fig. 7(b) and (c) shows the edge-detection results using both the Canny edge-detection method and the proposed algorithm. It is clear that the flame edges detected using the Canny edge-detection method are unclear and discontinuous, while the results obtained using the proposed algorithm show clear and continuous edges with parameters automatically adapted.

With a clearly defined flame/fire edge, various flame/fire parameters can be easily computed for the shape description. For instance, the flame area can be counted by the number of pixels inside the flame edge; the chain coding of a flame edge can be used to describe a 2-D flame/fire shape; the perimeter of a flame can be achieved by the total number of pixels of the detected flame edge boundary. Fig. 8 is an example of the uninterrupted computing of the flame perimeters from a flame video. It would be difficult to obtain this result without the clear edge detection. Using the proposed edge-detection algorithm, further work can be done to characterize the geometric features of flames/fires and, consequently, establish their relationship with combustion conditions such as air/fuel inputs and emissions.

To assess the antinoise effect of the algorithm, different types of random noise are added to the flame images before the images are processed. Fig. 9 shows an example of processing results with pepper and salt noise added. Fig. 9(b) is the flame edge detected from the original flame image in Fig. 9(a), while Fig. 9(d) shows the flame edge detected from the flame image with pepper and salt noise added. It can be seen that the shape

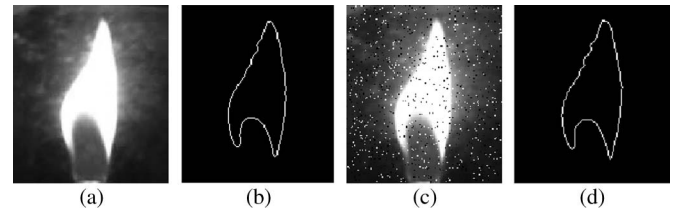


Fig. 9. Example of noisy and processed flame images. (a) Original image. (b) Processed image of (a). (c) Original image with salt and pepper noise added. (d) Processed image of (c).

detected in Fig. 9(d) is almost identical to the shape detected in Fig. 9(b).

## V. CONCLUSION

After the flame characteristics are analyzed, a new flame edge-detection method has been developed and evaluated in comparison with conventional methods. Experimental results have demonstrated that the algorithm developed is effective in identifying the edges of irregular flames. The advantage of this method is that the flame and fire edges detected are clear and continuous. Furthermore, with the change of scenarios, the parameters in the algorithm can be automatically adjusted. The clearly defined combustion region lays a good foundation for subsequent quantification of flame parameters [27], such as flame volume, surface area, flame spread speed, and so on. It is envisaged that this effective flame edge-detection algorithm can contribute to the in-depth understanding and advanced monitoring of combustion flames. Meanwhile, the algorithm provides a useful addition to fire image processing and analysis in fire safety engineering. The work presented was aimed for the processing of flame and fire images captured in laboratories. Further work is required to evaluate the performance of the algorithm in real-life flame detection scenarios.

## ACKNOWLEDGMENT

The views expressed are those of the authors and not necessarily those of the Research Councils U.K. (RCUK). The Energy Program is an RCUK cross-council initiative led by the Engineering and Physical Sciences Research Council and contributed to by Economic and Social Research Council, Natural Environment Research Council, Biotechnology and Biological Sciences Research Council, and Science and Technology Facilities Council.

## REFERENCES

- [1] D. Roddy, *Advanced Power Plant Materials, Design and Technology*. Cambridge, U.K.: Woodhead Publ., 2010.
- [2] G. Lu, Y. Yan, and M. Colechin, "A digital imaging based multi-functional flame monitoring system," *IEEE Trans. Instrum. Meas.*, vol. 53, no. 4, pp. 1152–1158, Aug. 2004.
- [3] Y. Yan, T. Qiu, G. Lu, M. M. Hossain, and G. Gilabertet, "Recent advances in 3D flame tomography," in *Proc. 6th World Congr. Ind. Process Tomogr.*, Beijing, China, Sep. 2010, pp. 1530–1539.
- [4] D. S. Huang, L. Heutte, and M. Loog, "Real-time fire detection using camera sequence image in tunnel environment," in *Proc. ICIC*, vol. 4681, LNCS, 2007, pp. 1209–1220.
- [5] Z. Zhang, J. Zhao, D. Zhang, C. Qu, Y. Ke, and B. Cai, "Contour based forest fire detection using FFT and wavelet," in *Proc. Int. Conf. CSSE*, Wuhan, China, Dec. 12–14, 2008, pp. 760–763.

[6] X. Zhou, F. Yu, Y. Wen, Z. Lu, and G. Song, "Early fire detection based on flame contours in video," *Inf. Technol. J.*, vol. 9, no. 5, pp. 899–908, 2010.

[7] B. U. Toreyin, Y. Dedeoglu, and A. E. Cetin, "Flame detection in video using hidden Markov models," in *Proc. IEEE ICIP*, Sep. 11–14, 2005, p. II-1230-3.

[8] B. U. Toreyin, Y. Dedeoglu, U. Gudukbay, and A. E. Cetin, "Computer vision based method for real-time fire and flame detection," *Pattern Recognit. Lett.*, vol. 27, no. 1, pp. 49–58, Jan. 1, 2006.

[9] M. I. Chacon-Murguia and F. J. Perez-Vargas, "Thermal video analysis for fire detection using shape regularity and intensity saturation features," in *Proc. MCPFR*, vol. 6718, *Lecture Notes in Computer Science*, 2011, pp. 118–126.

[10] S. M. Razmi, N. Saad, and V. S. Asirvadam, "Vision-based flame analysis using motion and edge detection," in *Proc. ICIAS*, no. Jun. 15–17, 2010, pp. 1–4.

[11] B. U. Toreyin and A. E. Cetin, "Online detection of fire in video," in *Proc. IEEE Conf. CVPR*, 2007, pp. 1–5.

[12] G. Lu, G. Gilabert, and Y. Yan, "Vision based monitoring and characterization of combustion flames," *J. Phys. Conf. Ser.*, vol. 15, no. 15, pp. 194–200, 2005.

[13] H. C. Bheemul, G. Lu, and Y. Yan, "Three-dimensional visualization and quantitative characterization of gaseous flames," *Meas. Sci. Technol.*, vol. 13, no. 10, pp. 1643–1650, Oct. 2002.

[14] B. C. Ko, K. H. Cheong, and J. Y. Nam, "Fire detection based on vision sensor and support vector machines," *Fire Safety J.*, vol. 44, no. 3, pp. 322–329, Apr. 2009.

[15] Q. Jiang and Q. Wang, "Large space fire image processing of improving canny edge detector based on adaptive smoothing," in *Proc. Int. CICC-ITOE*, 2010, pp. 264–267.

[16] C. W. Adkins, "Users guide for fire image analysis system-Version 5.0: A Tool for measuring fire behavior characteristics," U.S. Dept. Agric., Forest Service, Southern Res. Station, Asheville, NC, Gen. Tech. Rep. SE93, 1995.

[17] X. She and F. Huang, "Flame edge detection based on C–V active contour model," in *Proc. Int. Conf. Artif. Intell. Comput. Intell.*, 2009, vol. 2, pp. 413–417.

[18] R. C. Gonzalez and R. E. Woods, *Digital Image Processing*, 2nd ed. Englewood Cliffs, NJ: Prentice-Hall, 2002.

[19] T. Steinhaus, S. Welch, R. Carvel, and J. L. Torero, "Large-scale pool fires," *Thermal Sci. J.*, vol. 11, no. 3, 2007, special on fire.

[20] J. Canny, "A computational approach to edge detection," *IEEE Trans. Pattern Anal. Mach. Intell.*, vol. PAMI-8, no. 6, pp. 679–698, Nov. 1986.

[21] K. R. Castleman, *Digital Image Processing*. Englewood Cliffs, NJ: Prentice-Hall, 1995.

[22] SWRI, Small-scale liquid pool fire characterization. [Online]. Available: <http://www.swri.org/4org/d01/fire/firetech/about.htm>

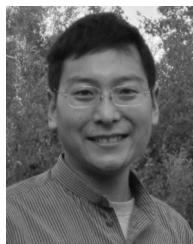
[23] D. Ziou and S. Tabbone, "Edge detection techniques: An overview," *Int. J. Pattern Recognit. Image Anal.*, vol. 8, no. 4, pp. 537–559, 1998.

[24] S. Haykin, *Adaptive Filter Theory*. Englewood Cliffs, NJ: Prentice-Hall, 2002.

[25] T. Qiu, Y. Yan, and G. Lu, "A new edge detection algorithm for flame image processing," in *Proc. IEEE I2MTC*, Hangzhou, China, May 10–12, 2011, pp. 281–284.

[26] W. S. Steven, *The Scientist and Engineer's Guide to Digital Signal Processing*. San Diego, CA: California Tech. Publ., 2003.

[27] T. Qiu, Y. Yan, and G. Lu, "A medial axis extraction algorithm for combustion flames through digital image processing," in *Proc. 6th ICIG*, Hefei, China, Aug. 12–15, 2011, pp. 182–186.



**Tian Qiu** received the B.Eng. degree in precision instrumentation and the M.Sc. and Ph.D. degrees in circuits and systems from the University of Science and Technology of China, Hefei, China, in 2000, 2003, and 2006, respectively.

He was an Engineer and a Senior Engineer with Samsung Electronics, Korea, from 2006 to 2009. He is currently a Research Associate with the Instrumentation, Control and Embedded Systems Research Group, School of Engineering and Digital Arts, University of Kent, Canterbury, U.K. His research interests include image processing, image analysis, and video processing.



**Yong Yan** (M'04–SM'04–F'11) received the B.Eng. and M.Sc. degrees in instrumentation and control engineering from Tsinghua University, Beijing, China, in 1985 and 1988, respectively, and the Ph.D. degree in solid flow measurement and instrumentation from Teesside University, Middlesbrough, U.K., in 1992.

In 1988, he started his academic career as an Assistant Lecturer with Tsinghua University. In 1989, he joined Teesside University as a Research Assistant. After a short period of postdoctoral research, he was initially a Lecturer with Teesside University

during 1993–1996 and then a Senior Lecturer, Reader, and Professor, respectively, with the University of Greenwich, London, U.K., during 1996–2004. He is currently a Professor of electronic instrumentation, the Head of Instrumentation, Control and Embedded Systems Research Group, and the Director of Research with the School of Engineering and Digital Arts, University of Kent, Canterbury, U.K. He has published in excess of 270 research papers in journals and conference proceedings in addition to 12 research monographs.

Dr. Yan is a Fellow of the Institution of Engineering Technology (IET) [formerly Institution of Electrical Engineers (IEE)], the Institute of Physics, and the Institute of Measurement and Control, U.K. He was a recipient of the Achievement Medal by the IEE in 2003, the Engineering Innovation Prize by the IET in 2006, and the Rushlight Commendation Award in 2009. In recognition of his contributions to pulverized fuel flow metering and flame imaging, he was named an IEEE Fellow in 2011.



**Gang Lu** (SM'05) received the B.Eng. degree in mechanical engineering from Central South University, Changsha, China, in 1982 and the Ph.D. degree in advanced combustion instrumentation from the University of Greenwich, London, U.K., in 2000.

He started his career as a Research Engineer and worked on mechanical design and engineering development for iron- and steel-making industry in China for more than ten years. He was a Postdoctoral Research Fellow with the University of Greenwich and the University of Kent, Canterbury, U.K., from 2000 to 2006. He is currently a Lecturer in electronics and instrumentation with the School of Engineering and Digital Arts, University of Kent. His main area of research is combustion instrumentation. He has been involved in a range of projects on advanced monitoring and characterization of fossil fuel flames.

Dr. Lu was a recipient of the Engineering Innovation Prize by the Institution of Engineering Technology, U.K., in 2006. He is a Chartered Engineer and a member of the Energy Institute (U.K.).